

Spatial cluster analysis of *Mycobacterium kansasii* infection in Kaohsiung, Taiwan

BO-CHEN LIU¹, HUNG-LING HUANG², TA-CHIEN CHAN³, SHIN-JUNG LEE⁴, JIUN-NONG LIN⁵,
CHEN-HSIANG LEE⁶, JANN-YUAN WANG⁷, PO-LIANG LU², HSIEN-HO LIN^{1,*}

Objectives: Owing to the high virulence of *mycobacterium kansasii* and the increasing incidence in Kaohsiung, the present study aimed to analyze the spatial pattern of *mycobacterium kansasii* infection in Kaohsiung. **Methods:** We applied the Moran's I to estimate the spatial pattern of incidence risk and to identify the cluster core. The core of the cluster was confirmed by the spatial relative risk function with contouring an infection hotspot that the location of the comparative group were randomly sampled from the address database. **Results:** The positive and significant spatial autocorrelation based on the incidence risk of the basic statistical area was illustrated by the significance map with the cluster core locating in Xiaogang district. The spatial relative risk function indicated two hotspots, one located across Qianjin district and Yancheng district, and the other mainly sat in Xiaogang district. All the significant spatial relative risk ranged from 1.54 to 2.27. **Conclusions:** Two hotspots indicated that the *mycobacterium kansasii* infection not homogeneously distributes in Kaohsiung City. Infection sources may have specific spatial patterns, yet the susceptible host probably has other tendencies too. Therefore, our results should be interpreted as a combination of all factors related to this infection. (*Taiwan J Public Health*. 2021;**40**(6):713-723)

Key Words: *Nontuberculous mycobacterium, Mycobacterium kansasii, Moran's I, spatial relative risk function, adaptive kernel density estimation*

¹ Institute of Epidemiology and Preventive Medicine, College of Public Health, National Taiwan University, No. 17, Xu-Zhou Rd., Zhongzheng Dist., Taipei, Taiwan, R.O.C.

² Division of Infectious Diseases, Department of Internal Medicine, Kaohsiung Medical University Hoasptial, Kaohsiung, Taiwan, R.O.C.

³ Center for Geographic Information Science, Research Center for Humanities and Social Sciences, Academia Sinica, Taipei, Taiwan, R.O.C.

⁴ Division of Infectious Diseases, Department of Internal Medicine, Kaohsiung Veterans General Hospital, Kaohsiung, Taiwan, R.O.C.

⁵ Division of Infectious Diseases, Department of Internal Medicine, E-Da Hospital, Kaohsiung, Taiwan, R.O.C.

⁶ Division of Infectious Diseases, Department of Internal Medicine, Kaohsiung Chang Gung Memorial Hospital, Kaohsiung, Taiwan, R.O.C.

⁷ Department of Internal Medicine, National Taiwan University Hospital, Taipei, Taiwan, R.O.C.

* Correspondence author
E-mail: hsienho@ntu.edu.tw

Received: Aug 9, 2021

Accepted: Nov 15, 2021

DOI:10.6288/TJPH.202112_40(6).110098



INTRODUCTIONS

In southern Taiwan, Huang and colleagues [1] observed a rising incidence rate of the nontuberculous mycobacteria pulmonary infection from 2010 to 2014, with an average incidence rate of 46 per 100,000 hospital-based patient-years, based on the hospital population of Kaohsiung Medical University hospital. They considered the increasing tendency mainly caused by the substantial rise between 2013 and 2014 for the *mycobacterium kansasii* (*M. kansasii*) episodes. Of the clinical feature, *M. kansasii* has a high virulence [2] and can cause indistinguishable clinical symptoms from the *mycobacterium tuberculosis* that increase the complexity of diagnosis. Fully understanding the infection hotspot could help target the causes of the transmission route, however, the spatial distribution of

the nontuberculous mycobacterium (NTM) pulmonary sample differed by region [3]. These findings indicated that the probability of getting an infection was dissimilar in a particular region, though all NTM species mentioned as the ubiquitous organism in the environment. Specifically, different NTM species may live in a specific natural niche [4]. Environmental sampling studies found that *M. kansasii* was widely prevalent in water, such as indoor swimming pools, city tap water, drinking water distribution system, but was rarely isolated from soil [5-7].

Several geospatial studies in the past reported the areas of the significant high-risk clusters of NTM infection in their study region [8-13]. However, these studies conducted a spatial analysis by pooling data into geographic areas, they utilized geographic centroid from their statistical areas to represent overall epidemiological estimates alternatively. Those results usually limited by administrative boundaries. Furthermore, analyzing the overall relationship across several species may obscure the association between a specific species and the environment. Because of the differences between NTM species, high pathogenic species need specific studies to clarify the features of their transmission.

Comprehensively understand the area which conducted to the transmission of *M. kansasii* is essential that can attribute to forming the cost-effective public health initiative to control the disease. Due to the high virulence [2] and the escalating *M. kansasii* episodes in Kaohsiung City, we aimed to conduct a multiple-hospital cohort study to detect the infection hotspot.

MATERIALS AND METHODS

Kaohsiung City is a coastal city and the third populous special municipality in

Taiwan. The population of the city is 2.77 million people and is administratively divided into 38 districts with an area of 2,952 square kilometers. We conducted the spatial cohort study based on all the city residence addresses as our study population between 2015 to 2017. Among the city population, there were 537 *M. kansasii* infected cases between these three years.

The study outcome of interest was incident culture-confirmed *M. kansasii*. All the new cases of *M. kansasii* in Kaohsiung between 2015 to 2017 were included. Four hospital systems included Kaohsiung Medical University Hospital (KMU), Kaohsiung Veterans General Hospital (KVGH), I-Shou University E-DA Hospital (EDAH), and Kaohsiung Chang-Gung Memorial Hospital (KCGMH) systems joined the collaboration.

All the culture-confirmed cases of *M. kansasii* were defined as conducting the Matrix-assisted laser desorption/ionization-time of flight (MALDI-TOF) spectrometry identification and also characterized by radiologic and pathologic diagnosis (follow American Thoracic Society/Infectious Diseases Society of America diagnosis criteria [14]). Since the divergent growing rate for the bacteria culturing would due to different culture managements, therefore, different laboratory confirmation may lead to differential misclassification of information bias. Before 2015, EDAH, KCGMH, and KMU applied different types of spectrometry identification. Four hospitals conducted the same MALDI-TOF microbiology diagnosis method after 2015. Thus we set the study time horizon from 2015 to 2017 to ensure the laboratory identifications upon these four hospitals were consistent. The representativeness of the observed cases can be held because patients from these hospitals should have enough coverage of *M. kansasii* infection in Kaohsiung City.

The exposure of interest in this study was the location of the residence. Infection sources of *M. kansasii* were generally thought to come from the water environment or water-related activities, but it was not feasible to locate and record where people were exposed to water sources. We, therefore, considered the residence as the most likely site of exposure alternatively.

There were two types of data for the exposure of interest: one was the residence of the observed cases between the study time horizon, another one was the general population's addresses. The residence address of the observed patients was retrieved from the medical records. In the contrast, addresses of the general population were simulated by sampling the address database [15] because the null hypothesis of the study assumed that individuals are randomly infected by a ubiquitously spreading *M. kansasii*. Places with high population density ought to have numerous cases. Thus we conducted the probability proportional to size (PPS) method by adjusting the village population to randomly sample four times the number of observed cases for the random infection location. All the Chinese addresses were checked and obtained both the complete address and its Taiwan geodetic datum 1997 (TWD97) coordinates from Taiwan Geospatial One Stop (TGOS) and the Kaohsiung City Doorplate Searching System.

We applied the global Moran's I [16] to measure the spatial autocorrelation on the incidence risks of the basic statistical area then further detected the hotspot core by the local Moran's I [17]. Subsequently, we conducted the spatial relative risk function [18] to depict the range of the hotspot.

The basic statistical area is the smallest geographic unit in Taiwan. Each area presents the highly homogeneous characteristics that makes the data at this geographic level

closer to the distribution of real situations. We integrated all the cases' locations into the basic statistical area that its population data came from the Ministry Of Interior Open Data system [19]. Then we measured the spatial autocorrelation of the area incidence risk by the global Moran's I. For the statistical testing, the transformation of the Moran's I to z-score evaluated the p-value for the significance. The global Moran's I range from -1 to +1. When the positive spatial autocorrelation is present, it means the basic statistical area with similar-high or -low incidence risk tends to gather together. Detection of the cluster core can be achieved by decomposing the global statistic. The local indicators of spatial association (LISA) evaluated whether each basic statistical area was related to its incidence risk with neighbors of the area. We further adjusted the result by the Bonferroni correction for reducing the likelihood of false-positive conclusions. All analyses of Moran's I were performed with the *spdep* package [20] by R version 3.6.1 [21].

The spatial relative risk function compared both the kernel density estimation (KDE) of the observed cases and the hypothetical infection. Let \hat{f} as the KDE of the observed cases and \hat{g} as the hypothetical KDE of the stochastically infected cases, $\hat{r} = \hat{f}/\hat{g}$ presented the spatial relative risk. In general, the spatial relative risk presented by taking the logarithm for the reason of treating two layers of observation symmetric.

$$\hat{\rho}(x) = \log \left[\frac{\hat{f}(x|X)}{\hat{g}(x|Y)} \right]$$

Where $X = \{x_1, x_2, \dots, x_n\}$ was the geographic coordinates of the observed cases, $Y = \{y_1, y_2, \dots, y_n\}$ was the coordinates of the random infection.

After getting a dividend of two densities, we test the null hypothesis for the independent locating of the observed cases by the upper tailed test with the equivalence of 1 (no

difference) or not. This approach using the z transformation to generate a spatial contour of p -value on statistical significance. In terms of the computational cost, we assigned a grids with 0.09 square kilometers for one density estimation.

The bandwidth in the kernel density determined the degree of smoothing, however, the distance between each location varied widely, therefore we applied the adaptive bandwidth into kernel density estimation since the adaptive bandwidth can catch the detailed information in the area with the dense population but also apply the larger bandwidth for the place where merely have the sparse observation.

The analysis of spatial relative risk conducted in two defined areas, one was the whole region of Kaohsiung City, another performed in a limited one. We focus on thirteen districts (Niaosong, Gushan, Sanmin, Yancheng, Xinxing, Qianjin, Lingya, Xiaogang, Qijin, Qianzhen, Fengshan, Daliao, and Linyuan District) of the urban area. Analyzed the spatial relative risk in the limited region can avoid getting a too-broad pilot bandwidth due to only a few cases located in the mountain area. We further performed the sensitivity analysis of spatial relative risk function for the different observed case and sampled case ratios (1:4 and 1:8) to test the uncertainty of the sampling process. All analyses of spatial relative risk function were conducted on R package sparr[22].

RESULTS

In 2015-2017, there were 537 cases diagnosed as *M. kansasii* infection. Case numbers of KMU, KVGH, EDAH, and KCGMH were 302, 59, 12, 164, respectively. The choropleth map of figure 1 showed the incidence risk of basic statistical area in Kaohsiung. The majority of cases were

attributed to the city center but one case located in the mountain-area.

The global Moran's I estimated the spatial autocorrelation for the incidence risk of the basic statistical area. The global index was 6.86×10^{-3} (p -value = 0.022). The value indicated that the basic statistical area with a similar incidence risk in Kaohsiung tended to cluster together. The global Moran's I elaborated that there existed a statistically significant clustered spatial pattern. The significance map of local Moran's I in figure 2 showed there were several cluster cores in Xiaogang district. The high-high clusters mean that the incidence risk of the area was significantly higher than the average incidence risk. In addition, its neighbors also had the same significant-high incidence risk. Areas surround the cluster center shall belonging to the high-risk cluster too.

In figure 3a, the heatmap included 537 observed cases and 2,148 sampled controls. There were three significant high-risk clusters, all of which located in the southwestern urban area of Kaohsiung City. Mountain districts have relatively big area but have rarer infection events than those with abundant case numbers in the urban area. When we only have a small sample size, the spatial relative risk function for the whole city may estimate an over-smooth global bandwidth that would cause a significant high-risk area to be too-broad. Because the mountain area has very few cases, we further redefined the analysis region in the southwestern urban area which included thirteen districts to get the finer high-risk area.

Figure 3b showed the result of the region redefined analysis. Two significant high-risk clusters were discovered. They mainly located at Qianjin-Yancheng district and Xiaogang district, respectively. The significant spatial relative risk ranged from 1.54 to 2.30. There were 16 and 35 cases included in Qianjin-Yancheng high-risk area and Xiaogang high-

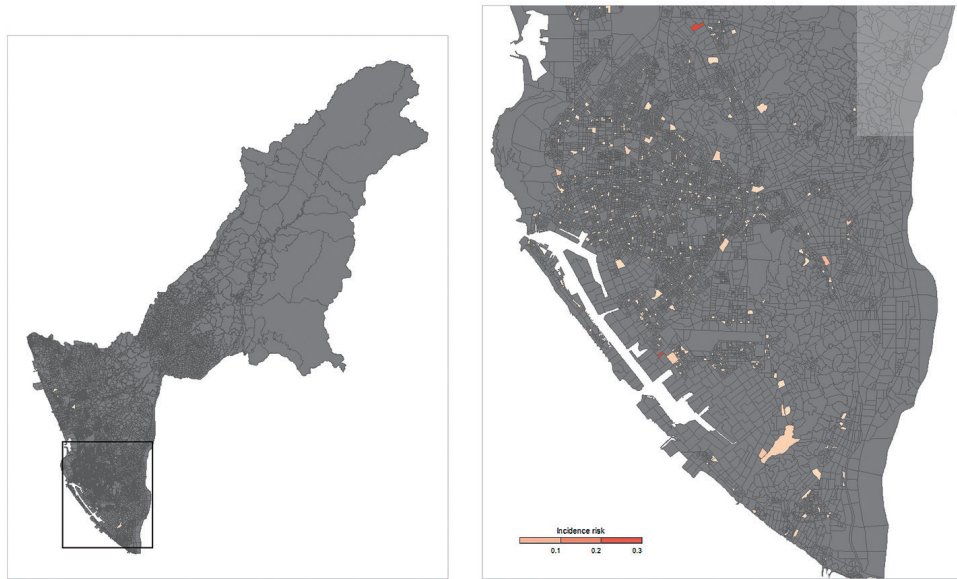


Figure 1. Incidence risk of basic statistical area in Kaohsiung City

Note: The incidence risk ranged from 0.0008 to 0.33. The basic statistical area with the highest incidence risk located in the Qianzhen district.

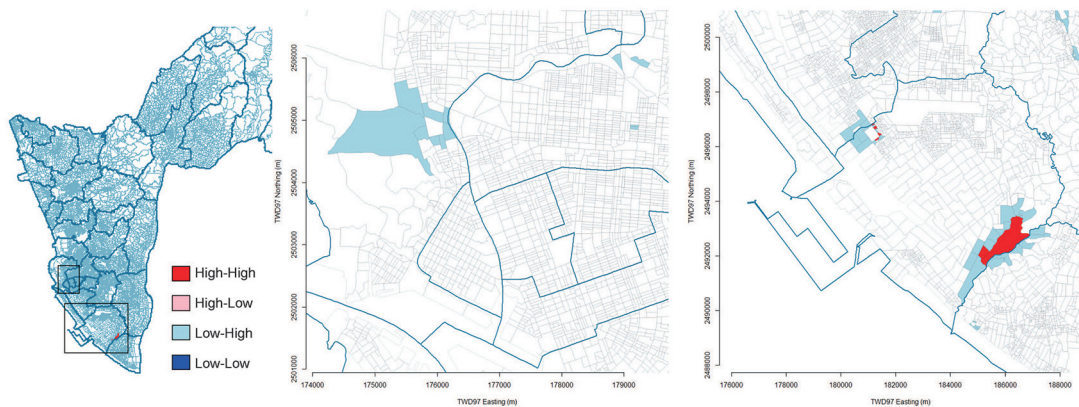


Figure 2. Significance map of local Moran's I for incidence risk of basic statistical area in Kaohsiung City

Note: The high-high cluster presented in red indicated the core of the cluster. The majority of the high-high clusters were in Xiaogang district. Red areas represented that they had the same high incidence risk as to its neighbors.

risk area, respectively. The results of the sensitivity analysis for randomly sampled locations from the address database showed the variation of hotspot contour in figure 4. The sampled addresses were four times and

eight times the number of the observed cases. Hotspots in Xiaogang district were detected in each spatial relative risk heatmap, though the location and the range varied by the sampling process. One western hotspot consistently

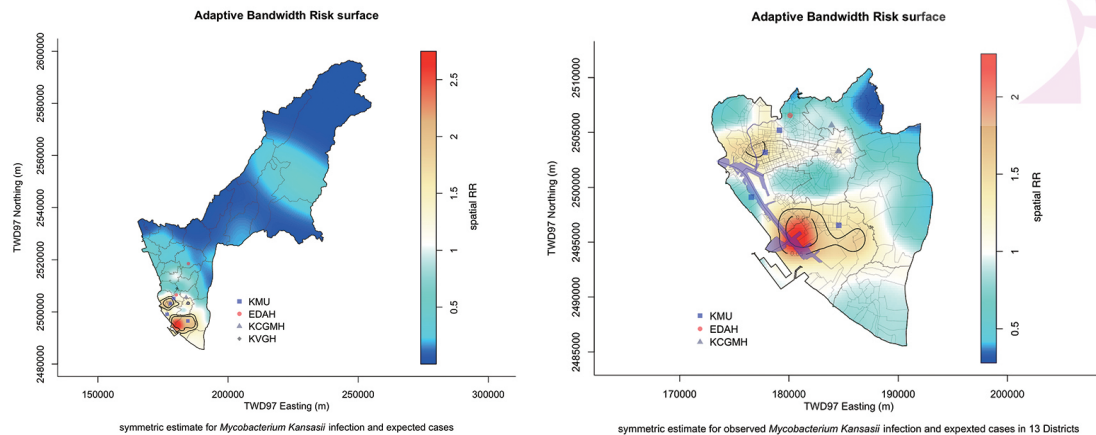


Figure 3. Heatplot of spatial relative risk for (a) *M. kansasii* infection, (b) *M. kansasii* infection in 13 defined region

Note: The unit of both two x and y axes was according to the TWD97 system. The gradient color scale represented the degree of the spatial relative risk. The higher the spatial relative risk is, the color would be deeper red, in contrast, deeper blue for the smaller value. The outer contour denotes the p-value being 0.05 and the inner contour represents the significance reach the p-value of 0.01. The slightly transparent blue area represented the Love River basin and the Kaohsiung port. Colored icons represented the location of the hospitals.

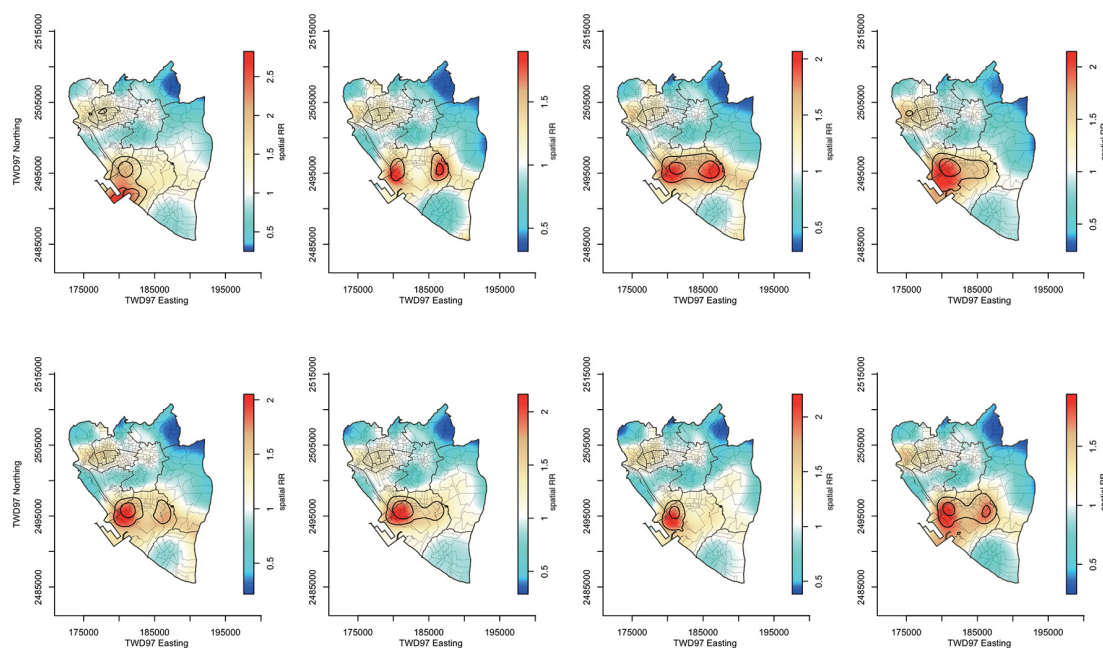


Figure 4. Sensitivity analysis of spatial relative risk function

Note: Sampled cases of the upper four heatplots were four times the numbers of observed cases; The lower four heatplots had eight times the numbers of the observed cases. All spatial relative risk represented in the gradient color scale with the inner and the outer contour line denoted for 0.01 and 0.05 p-values, respectively.

existed in Xiaogang district. Only two of the sensitivity heatplots had a significant high-risk area in the Qianjin-Yancheng district.

DISCUSSIONS

Generally, the utilization of a choropleth map is the most straightforward approach for targeting a suspected area with some epidemiological estimates. In figure 1, area with the highest incidence risk was in the Qianzhen district. But one addition of case count can amplify the incidence risk in an area with a small population. Hence the usage of the Moran's *I* with the spatial relative risk function, can not only grasp the spatial pattern but also describe a clear range of the high-risk hotspot.

In one population-based study in the U.S., Jennifer and her colleagues found the pulmonary NTM high-risk clusters significantly tended to have greater population density, median income levels, daily mean evapotranspiration, surface water proportion, soil sodium levels, and manganese levels. They also detected seven significant high-risk and five significant low-risk clusters for the pulmonary NTM cases by the spatial scan statistic, SaTScan [8]. Another study from Colorado [9] also applied SaTScan to identify clusters under the Zone Improvement Plan (ZIP) code level. They discovered two high-risk clusters in Colorado and adjusted environmental factors, sociodemographic factors, and population proportion by the Bayesian regression model. The authors concluded that older age, higher education, and low soil pH value were significant risk factors for increasing the risk of the slow-growing NTM disease.

However, both these results could only infer an NTM non-specific conclusion. The characteristics of different NTM infections are not all the same. Pooling all kinds of NTM

infections together is impractical to clarify the cause of the infection hotspot. Even, could give rise to ecological fallacy for a specific species. Previous studies generally used the data which combined several NTM species, therefore, to interpret their hotspots and its causes should consider those results as the integrated infection pattern. Furthermore, the disease pathogens and their hosts do not live according to the administrative boundary. The geographic level of data was also one of the limitations for previous analysis too. Studies utilized geographic centroid to represent the location of every not similar shape and size area will assume that cases are homogeneously distributing in each statistical area. The detailed spatial pattern and the explicit range of the hotspot which actually is across the administrative boundary cannot be clarified when the above-mentioned limitations exist.

An infection of NTM does not mandatorily report in many countries. The spatial pattern may be biased when the hospital's coverage of this disease is not high. If the majority of data come from one hospital or a single database, the results may have a relatively lower representativeness of the case number in the study area. Results from this data may even make the findings merely be the hospital service area or the database catchment area. Only in one study from the Australian state of Queensland where NTM infection has been mandatorily reported since the practicing of a nationwide tuberculosis control scheme [11]. Their results also showed a heterogeneous distribution of the relative risk for *M. kansasii* infection. In southern Queensland, there were 75 times significantly higher than average and geographically concentrated at the town Roma and its surroundings.

M. kansasii has been sampled from the drinking water distribution system [5,23,24] and even can survive nearing the water boiler

[25]. In the municipal area, domestic water from water treatment plants was also found more likely to promote the growth of NTM [26] due to the resistance to the disinfectant. In addition, occupations of heavy industry mentioned being one risk factor for the development of *M. kansasii* lung disease [27]. However, the formations of the detected high-risk hotspots may result from several factors. Risk factors of the host and the environmental factors may exhibit several kind of spatial distributions. Further, the human-environment interaction should also involve in the formation of the hotspots we discovered. Therefore, the detected hotspots of the present study should only be interpreted as a combined product of all factors related to this infection.

Strengths of this study involved the utilization of basic statistical area and the selection of the control in spatial relative risk function. Several limitations ensure each basic statistical area was highly homogeneous. Promised the spatial unit in the test of spatial autocorrelation unlikely to be biased. Moreover, the calculation of the incidence risk and the randomly sampled address adjusted the effect of the population density which may affect the case number in an area but also influence the formation of the hotspot. To reduce the selection bias of the general population, we excluded every address which was not registered as the residence in the sampling process. Under the concern that the spatial pattern of risk retrieved by the spatial relative risk function is a stochastic observation, we further conducted the permutation test for randomly reallocating the label on the location and estimated the test statistic proposed by Professor Hazelton [28]. The test returned the p-value being 0.0116 after 10,000 replications. It concluded that, under the significance level of 0.05, the spatial distribution of the observed *M. kansasii* infection was not identical to the

resampling distribution: relabeling the location would change the spatial pattern.

Since the clinical symptoms are not specific for *M. kansasii* with other mycobacterium infection, culture confirmation combined other diagnoses are recommended [7]. In addition, tuberculosis infection is mandatory in Taiwan, therefore, the confirmation coverage rate of NTM infection could benefit from the process of mycobacterium tuberculosis diagnosis. Hence, we believed data from four collaborative hospitals have enough representativeness to the comparison between the spatial pattern of observed and simulated cases.

Nonetheless, our study still limited by several limitation. The adaptive bandwidth would be adjusted with the distance between the points. An area with abundant cases would cause the point's bandwidth to be smaller, cases in the area with scarce neighbors may then result in the larger bandwidth to catch more spatial information. In the construction of the spatial relative risk function, the global bandwidth was estimated by pooled locations for both observed and expected cases for the conservative estimation. However, the adaptive bandwidth may not appropriate to represent the infection range for the same source of *M. kansasii*. Further, though four hospitals may collect the majority *M. kansasii* cases infection with this organism is not a mandatory disease in Taiwan. Thus we still cannot preclude the potential bias that we may omit some of the infection cases other than the included four hospitals.

The proportion of the observed cases from KMU hospital to the total observed cases was 56%, the majority of cases came from one single hospital may because doctors were more likely to diagnose the infection. Furthermore, Kaohsiung Municipal Siaogang Hospital which is one branch of KMU system locates in the east of the identified Xiaogang

high-risk hotspot (not located in the high-risk hotspot but the eastern notch). There are sixteen observed cases in the Qianjin-Yancheng high-risk hotspot. Among these cases, there were fourteen cases came from the KMU system. Also, we observed thirty-five infections in Xiaogang high-risk hotspot that thirty patients also came from this hospital system. However, the majority of cases' residence located in the downtown. The identified high-risk hotspot may represent as KMU hospital catchment area for *M. kansasii* infection if the detection bias exists. Otherwise, cases detected by KMU hospital may have enough representativeness for the southern city. The representativeness of the infection location may not be enough when the infection was not only happening in the residence.

Though we assumed the environmental niche of *M. kansasii* was constant and would not be varied by time in Kaohsiung City, increase the case numbers may still change the range of the high-risk hotspot. This hotspot may imply where the spatial cluster was but did not an exactly constant region, also was not likely to individually infer as the spatial characteristics of environmental factors, pathogen, or host.

Despite our results can raise the attention for the diagnosis of *M. kansasii* infection when a patient comes from the detected two high-risk hotspot, possible mechanisms for the infection were still unclear. Biological and phylogenetic evidence can help to enhance the confidence of the identification. Further research to investigate the infection sources of *M. kansasii* is needed. External evidence can not only promote the understanding of the species but also increase the suspicion of doctors for patients come from the high-risk hotspot with those risk factors. Further, initiate the prevention to decrease the disease burden of *M. kansasii*.

REFERENCE

1. Huang HL, Cheng MH, Lu PL, et al. Epidemiology and predictors of NTM pulmonary infection in Taiwan - a retrospective, five-year multicenter study. *Sci Rep* 2017;**7**:16300. doi:10.1038/s41598-017-16559-z.
2. van Ingen J, Bendien SA, de Lange WC, et al. Clinical relevance of non-tuberculous mycobacteria isolated in the Nijmegen-Arnhem region, The Netherlands. *Thorax* 2009;**64**:502-6. doi:10.1136/thx.2008.110957.
3. Hoefsloot W, van Ingen J, Andrejak C, et al. The geographic diversity of nontuberculous mycobacteria isolated from pulmonary samples: an NTM-NET collaborative study. *Eur Respir J* 2013;**42**:1604-13. doi:10.1183/09031936.00149212.
4. Honda JR, Virdi R, Chan ED. Global environmental Nontuberculous Mycobacteria and their contemporaneous man-made and natural niches. *Front Microbiol* 2018;**9**:2029. doi:10.3389/fmicb.2018.02029.
5. Engel HW, Berwald LG, Havelaar AH. The occurrence of *Mycobacterium kansasii* in tapwater. *Tubercle* 1980;**61**:21-6. doi:10.1016/0041-3879(80)90055-0.
6. Steadham JE. High-catalase strains of *Mycobacterium kansasii* isolated from water in Texas. *J Clin Microbiol* 1980;**11**:496-8. doi:10.1128/jcm.11.5.496-498.1980.
7. Akram SM, Rawla P. *Mycobacterium Kansasii*. Treasure Island, FL: StatPearls Publishing; 2021.
8. Adjemian J, Olivier KN, Seitz AE, Falkinham JO 3rd, Holland SM, Prevots DR. Spatial clusters of nontuberculous mycobacterial lung disease in the United States. *Am J Respir Crit Care Med* 2012;**186**:553-8. doi:10.1164/rccm.201205-0913OC.
9. Lipner EM, Knox D, French J, Rudman J, Strong M, Crooks JL. A geospatial epidemiologic analysis of Nontuberculous Mycobacterial infection: an ecological study in Colorado. *Ann Am Thorac Soc* 2017;**14**:1523-32. doi:10.1513/AnnalsATS.201701-081OC.
10. Rocha D, Felgueiras Ó, Duarte R. Can environmental determinants explain Nontuberculous Mycobacteria geographic incidence? *Pulmonology* 2020;**26**:145-50. doi:10.1016/j.pulmoe.2019.12.003.
11. Chou MP, Clements AC, Thomson RM. A spatial epidemiological analysis of nontuberculous mycobacterial infections in Queensland, Australia. *BMC Infect Dis* 2014;**14**:279. doi:10.1186/1471-2334-14-279.
12. Modra H, Ulmann V, Caha J, et al. Socio-economic and environmental factors related to spatial

- differences in human Non-Tuberculous Mycobacterial diseases in the Czech Republic. *Int J Environ Res Public Health* 2019;**16**:3969. doi:10.3390/ijerph16203969.
13. Adjemian J, Olivier KN, Prevots DR. Nontuberculous mycobacteria among patients with cystic fibrosis in the United States. *Am J Respir Crit Care Med* 2014;**190**:581-6. doi:10.1164/rccm.201405-0884OC.
14. Griffith DE, Aksamit T, Brown-Elliott BA, et al. An official ATS/IDSA statement: diagnosis, treatment, and prevention of nontuberculous mycobacterial diseases. *Am J Respir Crit Care Med* 2007;**175**:367-416. doi:10.1164/rccm.200604-571ST. Erratum in: 2007;**175**:744-5. Dosage error in article text.
15. Chien CT. House number-based sampling service. Available at: <https://sample.geohealth.tw/>. Accessed November 9, 2019. [In Chinese]
16. Moran PA. Notes on continuous stochastic phenomena. *Biometrika* 1950;**37**:17-23. doi:10.2307/2332142.
17. Anselin L. Local indicators of spatial association - LISA. *Geogr Anal* 1995;**27**:93-115. doi:10.1111/j.1538-4632.1995.tb00338.x.
18. Davies TM, Hazelton ML. Adaptive kernel estimation of spatial relative risk. *Stat Med* 2010;**29**:2423-37. doi:10.1002/sim.3995.
19. 國家發展委員會：政府資料開放平台。 <https://data.gov.tw/dataset/18681>。引用2019/11/07。 National Development Council. Open Government Data Platform. Available at: <https://data.gov.tw/dataset/18681>. Accessed November 7, 2019.
20. Bivand RS, Wong DWS. Comparing implementations of global and local indicators of spatial association. *Test* 2018;**27**:716-48. doi:10.1007/s11749-018-0599-x.
21. R Development Core Team. R foundation for statistical computing, Vienna, Austria. Available at: <https://www.R-project.org/>. Accessed August 9, 2021.
22. Davies TM, Marshall JC, Hazelton ML. Tutorial on kernel estimation of continuous spatial and spatiotemporal relative risk. *Stat Med* 2018;**37**:1191-221. doi:10.1002/sim.7577.
23. Thomson RM, Carter R, Tolson C, Coulter C, Huygens F, Hargreaves M. Factors associated with the isolation of Nontuberculous mycobacteria (NTM) from a large municipal water system in Brisbane, Australia. *BMC Microbiol* 2013;**13**:89. doi:10.1186/1471-2180-13-89.
24. Fischeder R, Schulze-Röbbecke R, Weber A. Occurrence of mycobacteria in drinking water samples. *Zentralbl Hyg Umweltmed* 1991;**192**:154-8.
25. Vaerewijck MJ, Huys G, Palomino JC, Swings J, Portaels F. Mycobacteria in drinking water distribution systems: ecology and significance for human health. *FEMS Microbiol Rev* 2005;**29**:911-34. doi:10.1016/j.femsre.2005.02.001.
26. Falkinham JO 3rd, Norton CD, LeChevallier MW. Factors influencing numbers of *Mycobacterium avium*, *Mycobacterium intracellulare*, and other *Mycobacteria* in drinking water distribution systems. *Appl Environ Microbiol* 2001;**67**:1225-31. doi:10.1128/AEM.67.3.1225-1231.2001.
27. Kim JH, Seo KW, Shin Y, et al. Risk factors for developing *Mycobacterium kansasii* lung disease: a case-control study in Korea. *Medicine (Baltimore)* 2019;**98**:e14281. doi:10.1097/MD.00000000000014281.
28. Hazelton ML. Testing for changes in spatial relative risk. *Stat Med* 2017;**36**:2735-49. doi:10.1002/sim.7306.

台灣高雄市堪薩斯分枝桿菌之空間分析

劉柏辰¹ 黃虹綾² 詹大千³ 李欣蓉⁴
林俊農⁵ 李禎祥⁶ 王振源⁷
盧柏樑² 林先和^{1,*}

目標：由於堪薩斯分枝桿菌的高致病性及高雄逐年上升的發生率，本研究旨在探討高雄堪薩斯分枝桿菌感染者之空間分佈及該菌種之感染熱區範圍。**方法：**利用高雄市2015至2017年間堪薩斯分枝桿菌感染者之地理資訊，以最小統計區為空間單位，藉莫蘭指數分析發生率之空間分佈型態及顯著的群聚核心。並隨機抽樣門牌地址以代表空間上均質的感染分佈，再透過空間相對風險函數比較感染者與隨機感染之座標來計算感染熱區的確切範圍。**結果：**發生率於最小統計區下之空間自相關呈顯著正相關（呈群聚趨勢），且顯著地圖指出群聚核心位於小港區內。空間相對風險分析亦得出兩感染熱區，分別位於前金、鹽埕區的交界及小港區內部（空間相對風險落在1.54至2.27之間）。**結論：**高雄市堪薩斯分枝桿菌感染者的分布並非均質，且存在感染熱區。然而感染來源與易感染人群的空間分布均可能有其特定的群聚趨勢，故本研究的結果應解讀為可能影響此感染症的所有因素在空間上的綜合表現。未來仍須更多生物與環境上的證據以佐證本研究之結論。（台灣衛誌 2021；40(6)：713-723）

關鍵詞：非結核分枝桿菌、堪薩斯分枝桿菌、莫蘭指數、空間相對風險函數、核密度估計

¹ 國立台灣大學公共衛生學院流行病學與預防醫學研究所

² 高雄醫學大學醫院內科部感染科

³ 中央研究院人文社會科學研究中心地理資訊科學研究專題中心

⁴ 高雄榮民總醫院內科部感染科

⁵ 義大醫院內科部感染科

⁶ 高雄長庚紀念醫院內科部感染科

⁷ 國立台灣大學醫學院附設醫院內科部

* 通訊作者：林先和

地址：台北市中正區徐州路17號

E-mail：hsienho@ntu.edu.tw

投稿日期：2021年8月9日

接受日期：2021年11月15日

DOI:10.6288/TJPH.202112_40(6).110098

評論：台灣高雄市堪薩斯分枝桿菌之空間分析

過去由於菌種鑑定困難、確診門檻高、且警覺性不如結核病，非結核分枝桿菌（Nontuberculous *Mycobacteria*）造成的感染容易被忽略。近年由於醫界宣導教育與質譜儀在臨床微生物鑑定的大量應用，台灣的非結核分枝桿菌診斷率逐漸攀升。其中，*Mycobacterium kansasii*為非結核分枝桿菌中常見致病源之一，常造成肺部疾患、皮膚軟組織感染、或者在免疫不全病患上造成全身性感染。

不同非結核分枝桿菌有其適合棲息的環境，過去文獻指出非結核分枝桿菌感染者常居住於某些地區，有學者便懷疑特殊的環境/供水系統可能成為感染源，本研究[1]探討2015年到2017年間高雄之*M. kansasii*病人是否都集中居住在某些區域（熱區），以及這些熱區的範圍涵蓋到何處。本研究擷取高雄主要醫院診斷的*M. kansasii*病人之居住地理位置，並考慮一般民眾居住密度，以global Moran's I來檢驗空間自相關（spatial autocorrelation），認為有些區域的發生率較高，再以Local Moran's I偵測盛行率高的熱區為小港區。研究再利用空間相對風險函數（spatial relative risk function）驗證熱區，並界定其範圍在小港以及前金/鹽埕交界處。

本研究可以提供公衛端著手調查的方向，但讀者不應理解為「該處環境或水源有問題，而造成當地*M. kansasii*發生率高」。對於高致病病原體，如霍亂、傷寒等，其宿

主因素影響較小，或許可以如此解釋，但是*M. kansasii*的感染與診斷常與宿主因素，如患者共病、社經地位、就醫習慣/頻次有關，舉例來說，若某區肺病盛行率較高，附近又有醫院，該區*M. kansasii*發生率應會較高。此研究結果可用以及早辨識高發生熱區，但仍需要以更精確的公衛調查與分析，考量干擾因子，方能找出確切原因，並進行後續有效介入。若懷疑有環境感染源，也應採檢後進行分子生物學比對，方能確認。

非結核分枝桿菌的感染非法定傳染病，其研究與調查多為醫界或學界主動發起，本研究即為公衛專家與醫界合作之成果。同時也揭示台灣大數據的搜集與公開的重要性，如文中提到的「國土資訊圖資服務平臺」與「全國及各縣市之最小統計區」等地理資訊，為本研究或相關研究不可或缺的基礎工具。

綜合上述，本研究欲驗證*M. kansasii*是否會有好發熱區，與醫院合作辨識出高雄病例高發生熱區，而高發生率實際原因尚待調查，但研究成果可為後續調查指明方向，方可進行有效的介入措施。

參考文獻

1. Liu BC, Huang HL, Chan TC, et al. Spatial cluster analysis of *Mycobacterium kansasii* infection in Kaohsiung, Taiwan. *Taiwan J Public Health* 2021;**40**:713-21. doi:10.6288/TJPH.202112_40(6).110098.

郭書辰

國家衛生研究院感染症與疫苗研究所

地址：苗栗縣竹南鎮科研路35號

E-mail: sckuo@nhri.edu.tw

DOI:10.6288/TJPH.202112_40(6).11009801